Soft Magnetic Materials,

Investigation on the soft-magnetic properties of CoZrTaB laminated cores by dielectric layer tuning

Guannan Wei[1], Rajasree Das[1], Daniel Lordan[1], Marek Lorenc[1], Barry Clarke[3], David P F Hurley[3], Mike Hayes[1], Cian O'Mathuna[1,2]**, Ranajit Sai[1], and Paul McCloskey[1]

[1] *Tyndall National Institute, University College Cork, Cork, T12 R5CP, Ireland*
[2] *School of Engineering, University College Cork, Cork, T12 HW58, Ireland*
[3] *TEL (Tokyo Electron) Magnetic Solutions Ltd, Dublin 9, D09 Y271, Ireland*
*** Fellow, IEEE*

Received xxx, revised xx, accepted xx, published xx, current version xx. (Dates will be inserted by IEEE; “published” is the date the accepted preprint is posted on IEEE Xplore®; “current version” is the date the typeset version is posted on Xplore®).

Abstract—Soft magnetic properties of thin films for use as a core material are critical for the realization of future miniaturized electromagnetic devices operating at frequencies of tens or hundreds MHz. Laminated stacks consisting of alternate thin layers of magnetic material and dielectric material are widely used to suppress eddy current losses that dominate especially at a higher frequency of operation. Thus, identifying a suitable dielectric layer, its optimum thickness, and the understanding of its effect on the performance of the laminated core is important. In this paper, six different CoZrTaB (CZTB) laminated cores are reported featuring a variety of dielectric materials (AlN, SiN, Al_2O_3, and oxide CZTB) and/or dielectric thickness (5, 15, and 50 nm). This study shows that stacks with different dielectric material have a varied residual stress that plays an important role in inducing magnetic anisotropy, thus affecting the permeability. CZTB stacks with oxide CZTB dielectric show the best combination of high permeability, low coercivity, and low losses at high frequency.

Index Terms—Magnetics on silicon, thin-film technology, soft magnetic laminated stacks, dielectric material.

I. INTRODUCTION

Thin magnetic film based integrated micro-inductors play a crucial role in applications ranging from wireless communication systems to integrated voltage regulators (IVRs) [O´Mathuna 2012, Lambert 2020]. The quest of miniaturization demands the inductors operate efficiently in the MHz frequency range. Large inductance-density, low loss, and good high frequency response are required for these applications. This provides research challenges not only in the optimization of device designs but also the improvement of the high frequency performances of the magnetic core material.

The design of magnetic cores in order to reduce the losses has attracted a great amount of attention in electrical application fields [Ikeda 2006, Fergen 2002]. Eddy currents and hysteresis losses are the contributing factors of the high-frequency losses of the magnetic core material. Hysteresis loss accompanied with magnetic domains that could result in localized magnetization resonances that, in turn, lead to more energy losses [Dinulovic 2020]. Eddy current induced by the time varying magnetic fields in the core, become the dominant loss contributor at high (above tens of MHz) frequencies [Wang 2017]. Laminated structures, consisting of multiple thin magnetic layers separated by dielectric films have been shown to stem the eddy-current losses successfully, and hence reduce the overall high frequency losses and improve the quality factor (Q-factor) [Wu 2012, Yao 2013] of the micro-inductors. Thus, the design and development of laminated magnetic core has become a significant activity towards developing efficient and miniaturized micro-inductors. Identifying a suitable dielectric layer and understanding its effect on the performance of the laminated core is an important part of this development.

Sputtered soft-magnetic laminates comprised of NiFe or Co-based amorphous alloys are popular for the on-chip integration at the CMOS back-end-of-line (BEOL) process [O´Mathuna 2012, Masood 2018]. A variety of dielectric materials such as AlN [Jordan 2021], Al_2O_3 [Michel 2019], SiO_2 [Dinulovic 2020], SiN [Bharadwaj 2017], and Co-based oxide [Raju 2020] are used in the laminates. One key feature, beside soft magnetic properties, that determines the success of the laminates commercially is their wet-etching capability. Stacks with AlN, Al_2O_3 are not easily patternable with large undercuts by a wet etching process. Whereas the preferred etchants for SiO_2 and SiN are HF or KOH based solution [Pal 2021], which are not conducive to BEOL processing. Recently, oxide of CZTB (O-CZTB), also investigated in this study, exhibits excellent CMOS compatibility with superior wet-etching capability than the state-of-the-art AlN [Wei 2023]. The investigation of the effect of different dielectric materials on the soft magnetic properties of the laminated stacks of CZTB using the same magnetic material sputtering conditions has not been previously reported.

In this work, six different CoZrTaB (CZTB) laminated cores were fabricated and characterized, comprising four different dielectric materials together with three different dielectric layer thicknesses for one of the dielectric materials. Amorphous ferromagnetic CZTB alloy film was chosen as the magnetic film of the laminates owing to its relatively higher resistivity of 120 μΩ·cm than the popular NiFe [Wang 2021] or CoZrTa [Michel 2019]. The effect of mechanical

Corresponding author: guannan.wei@tyndall.ie & ranajit.sai@tyndall.ie
Digital Object Identifier: 10.1109/LMAG.XXXX.XXXXXXX (inserted by IEEE).

stress in the fabricated laminates on the hysteresis and high-frequency losses was investigated in depth to identify the best suited dielectric layer for CZTB-based laminates.

II. EXPERIMENTAL DETAILS

A. Fabrication of the laminates

Amorphous CZTB(100 nm) /[dielectric (*x* nm)/CZTB(100 nm)]×9 laminates (*x* is dielectric layer thickness) were deposited by magnetron sputtering. Two groups of comparison studies were designed: one with the same dielectric layer thickness of 5 nm but different dielectric material (AlN, Al_2O_3, SiN and oxide of CZTB); the other using the same dielectric material oxide of CZTB (O-CZTB hereafter) but with the thickness varied from 5 nm to 50 nm.

Amorphous $Co_{84}Zr_4Ta_4B_8$ (at. %) target was used to grow the magnetic layer using DC magnetron sputtering (Lesker PVD model CMS-18HV system). The sputtering chamber was pumped down to a base pressure of 10^{-7} Pa, and then argon gas was introduced resulting in a sputtering pressure of 5 mTorr to start deposition of the CZTB magnetic films under the DC power of 500 W. The deposition of the films was carried out in an applied magnetic field of 230 Oe with homogeneous distribution across a 4-inch Si (100) wafer. The Si substrate was pre-processed to have a thermally grown SiO_2 layer of 250 nm followed by a 20-nm thick sputtered-deposited adhesion layer of Ti on top of it before the deposition of the magnetic films.

The dielectric AlN separation layers were deposited at 5 mTorr Ar atmosphere using AlN sputter target. Once the chamber pressure was stabilized, AlN was deposited for required time with the target power of 140 W. The Al_2O_3 dielectric films were deposited using an aluminum dioxide target under RF power supply with 140 W in an inert atmosphere. High purity (~99.99%) silicon target was used for the deposition of SiN film. RF power supply with 30% reactive N_2 gas and 35 W RF substrate bias was set for the deposition. In addition to the familiar dielectric materials, here we have optimized the deposition of a relatively new dielectric material, O-CZTB. Three O-CZTB films with different thicknesses (5, 15 and 50nm) were deposited by the reactive sputtering from the CZTB target under appropriate O_2 gas partial pressure. Detailed deposition conditions are published in our earlier work [Wei 2023].

B. Characterization methods

The structural properties of the films were investigated by X-ray diffraction (XRD, Philips Xpert diffractometer, Cu Kα-1.54 Å). Divergent beam setting was used during all the measurements to detect the tiny crystalline phase(s) if any. Surface roughness was characterized using AFM (Bruker Dimension Icon). The KLA Tencor P-17 stylus profilometer was used to measure the stress profile. The soft magnetic properties were investigated using a B-H hysteresis loop tracer (SHB, MESA 200 HF) at room temperature. The high-frequency (3 MHz – 4 GHz) permeability of films was measured using 4 mm × 4 mm samples by employing Ryowa PMM-9G Permeameter.

III. RESULTS AND DISCUSSION

A. Structural analysis

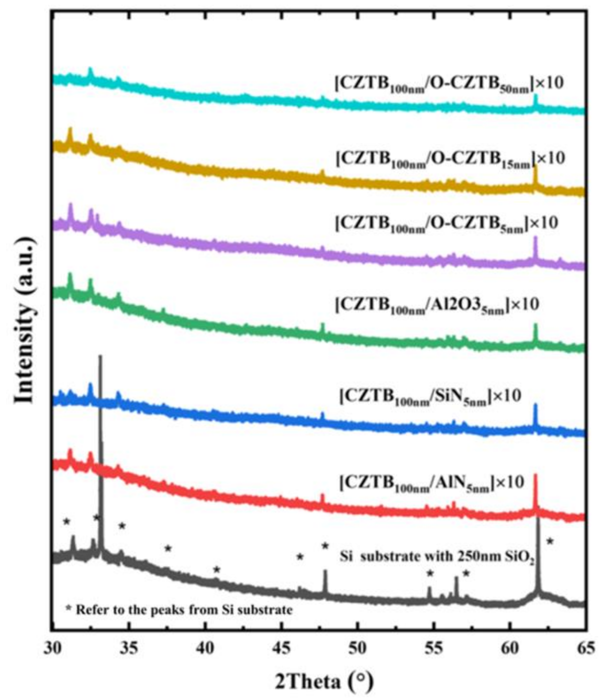

Fig. 1. XRD spectra of a bare Si-wafer with 250nm SiO2 (before film deposition), as-deposited CZTB lamination stack with dielectric material of AlN, Al_2O_3, SiN, and O-CZTB

Table 1. Summary of the characterization results of CZTB laminated stacks with different dielectric material or thickness.

Lamination structure	$[CZTB_{100nm}/Dielectric_{x\,nm}]\times10$					
Dielectric (Layer thickness)	AlN (5 nm)	SiN (5 nm)	Al_2O_3 (5 nm)	OCZTB (5 nm)	OCZTB (15 nm)	OCZTB (50 nm)
Stack stress (GPa)	+0.309	-0.04	+0.15	+0.115	+0.28	+0.32
Dielectric Rq (nm)	0.325	0.59	0.42	N.A.	0.49	0.67
Coercivity, Hc (A/m)	9.40	97.8	81.09	9.17	57.3	128
Anisotropy field (kA/m)	1.968	1.384	1.464	1.623	1.859	1.890
μ_r' @100 MHz	438	648	686	581	432	476
Q-factor @ 100 MHz	28.1	17.0	14.7	17.4	23.4	31.2
Magnetic flux density, B_s (Wb/m^2)	1.28	1.20	1.31	1.26	1.25	1.25

Physical structures of CZTB lamination stack with different dielectric materials or thickness (AlN, Al_2O_3, SiN, and O-CZTB) sputtered on Si/SiO_2 wafer were analyzed using XRD technique. Amorphous materials are favored in a soft magnetic core for high frequency inductor applications, due to lower coercivity, and lower magnetostriction than crystalline materials [O´Mathuna 2012]. Without magnetic crystalline anisotropy, it is easier to induce uniaxial anisotropy in amorphous materials and hence achieve better soft magnetic properties with low losses at high frequency [Nosenko 2020]. With proper sputtering condition optimization [Lordan 2021], an amorphous phase is achieved. Fig. 1 shows the spectrum 2θ scan pattern of samples along with a reference Si/SiO_2 substrate. In this work, p-type silicon wafer was used, then 250nm SiO_2 were thermally grown on top as insulation layer. XRD scans were performed before and after CZTB system sputtering, so that the peaks can be separated from the substrate and that from the CZTB films. The broad area in the range of 2θ=40-50° confirms the amorphous nature of all the films. The sharp peaks appearing in the range of 30°< 2θ<65° are from the substrate (marked with star symbols in the reference substrate sample).

B. Static magnetic characterization

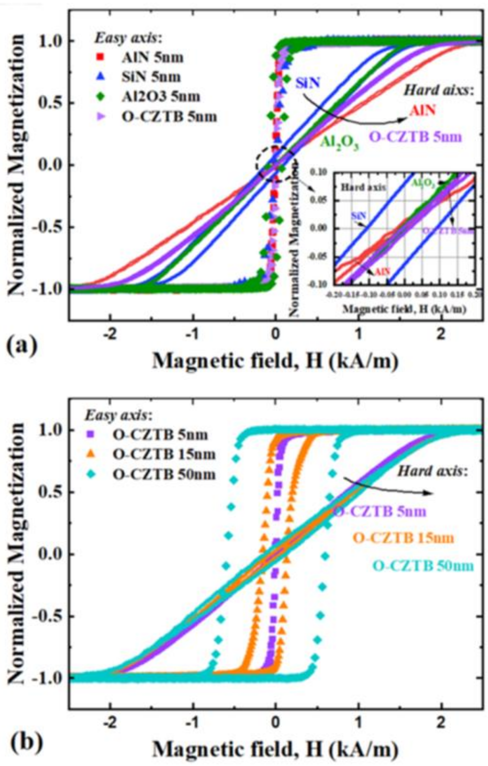

Fig. 2. Hysteresis loop of as-deposited CZTB lamination stack with dielectric material of a) AlN 5nm, Al_2O_3 5nm, SiN 5nm and O-CZTB 5nm; b) that of O-CZTB 5nm, 15nm, and 50nm.

Fig. 2 shows the easy and hard magnetic anisotropy axis hysteresis loops of the CZTB multilayer films dielectric material AlN 5nm, Al_2O_3 5nm, SiN 5nm, O-CZTB 5nm, O-CZTB 15nm, and O-CZTB 50nm. Uniaxial magnetic anisotropy was successfully induced on all the as-deposited samples with a low hard axis coercivity (H_c < 130 A/m). A pronounced magnetic anisotropy will result in coherent magnetic rotation during high frequency excitation, and hence is very beneficial in order to have the material working at high frequency with low losses. Magnetic anisotropy field (H_k) strength can be abstracted using Stoner-Wohlfarth model [Dubuget 2010] considering a single anisotropy model. Table 1 summarizes the coercivity (H_c) along hard axis, H_k values for all the samples together with the dielectric layer's roughness and the residual stress of laminated stack. It can be observed that 1) CZTB laminated stacks (5nm dielectric layer) with SiN has the largest H_c; 2) For stacks with O-CZTB, when dielectric thickness increases, the roughness increases so as H_c. The magnetic flux density (B_s) of each sample were also listed in table 1, where the CZTB system with SiN dielectric material has the lowest value, then the one with O-CZTB dielectric, where that with AlN and Al_2O_3 has the highest value.

Fig. 3 a) plotted the relationship between dielectric roughness and hard axis H_c. A positive correlation can be observed between the dielectric roughness and hard axis H_c. Film roughness can introduce surface irregularities disrupting the uniformity of the magnetic domain structure, which can lead to domain wall pinning or increased domain wall energy *[Ghaferi 2020, Jordan 2020]*. This in turn will result in an increase in coercivity, as more energy is required to initiate domain wall motion and magnetization reversal. Choosing the dielectric material with a lower roughness can lead to smaller H_c hence lower hysteresis losses. When dielectric thickness is the same (5nm), AlN or O-CZTB show the smallest H_c value.

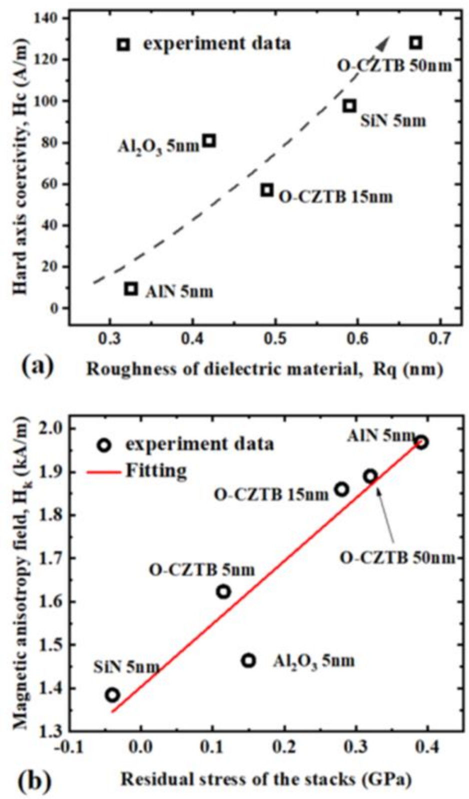

Fig. 3. a) Relationship of dielectric layer's roughness with hard axis coercivity; b) Relationship of residual stress of the stack and magnetic anisotropy field.

Fig. 3 b) plotted the relationship between the stack residual stress and H_k value. Likewise, it can also be observed that higher induced magnetic anisotropy H_k shows a positively proportional trend to the residual stress of stack samples. Stress can induce anisotropy via changing the preferential alignment of magnetic moments along specific directions during sputtering. Even though CZTB material's magnetostatic coefficient is low [Masood 2018, Cronin 2020], when the sputtering condition is the same, the stress induced anisotropy field will add to the intrinsic magnetic anisotropy (that induced by external magnetic field during sputtering) and influences the overall magnetic behavior of the laminated stacks samples with different dielectric material. A simple linear model can be generated here to fit the experimental date:

$$H_k = H_{k\_stress} + H_{k\_ini} = \zeta_{stress} * \sigma_{Stress} + H_{k\_ini},$$

where H_{k_stress} refer to the stress induced anisotropy, H_{k_0} is the initial anisotropy value generated by sputtering condition, σ_{Stress} is the residual stress, and ζ_{stress} is the stress related constant coefficient.

The fitting results show that H_{k_ini} = 1.404 kA/m, and ζ_{stress}=1.452 kA/(m·GPa) .

Anisotropy field H_k can be used to estimate the initial permeability (will be discussed in the next section C), with a smaller H_k value generating a higher permeability. Selecting the proper dielectric material or thickness can further tune the H_k via different residual stress. CZTB laminated stacks (same dielectric thickness) with SiN or Al_2O_3 show the lowest H_k value, O-CZTB is with medium value, while that with AlN has the largest H_k. When dielectric material is the same, as dielectric thickness decreases, the H_k also decreases. In summary, from the static magnetic study, it can be seen that CZTB laminated stack with 5nm O-CZTB dielectric has the lowest H_c and relatively smaller H_k.

C. High frequency permeability spectra

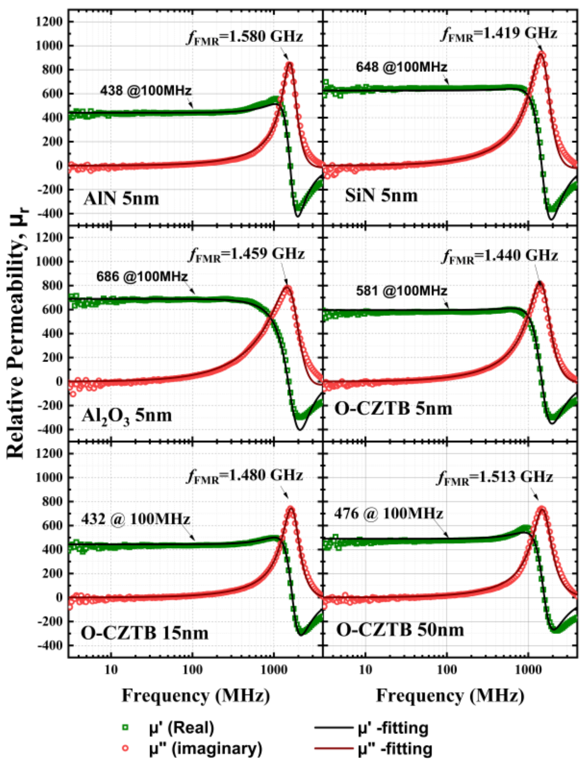

Fig. 4. High frequency permeability spectra of as-deposited CZTB lamination stack with dielectric material of AlN 5nm, Al2O3 5nm, SiN 5nm and O-CZTB 5nm (and 15nm, 50nm).

Frequency dispersion of complex permeability $\mu(f)$ spectra of all the samples are shown in Fig. 4, with μ' representing the real part while μ'' the imaginary part. It can be observed that the real part of the permeability of all samples holds flat until frequency as high as 300 MHz, indicating those magnetic core can be easily used at 100MHz working frequency. CZTB stack samples with SiN, or Al_2O_3 have the highest permeability at 100 MHz, while their H_k is the lowest. Likewise, CZTB stacks with AlN show lowest permeability but highest H_k. The inverse relationship between permeability and H_k can be explained by the estimation of static initial permeability using the expression of μ_{ini}=1+4πM_s/H_k [Seemann 2010], indicated in Fig. 5 a).

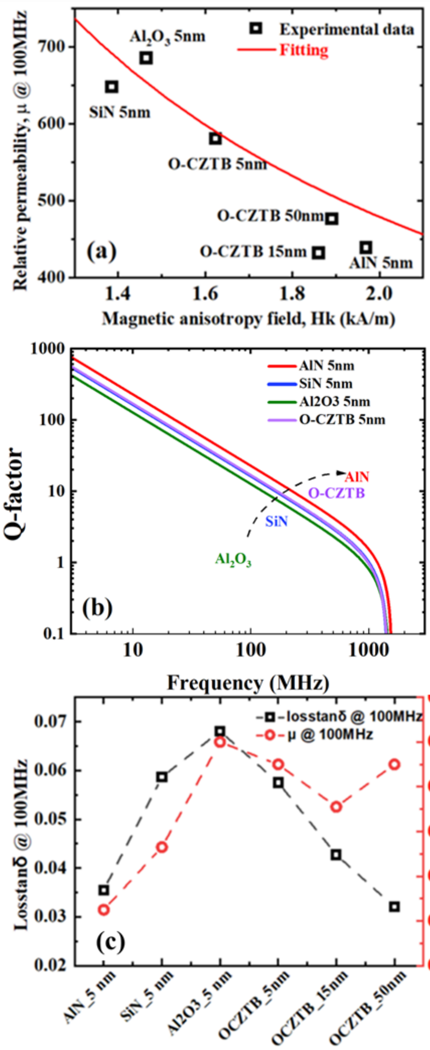

Fig. 5. a) Plotting of relative permeability (@ 100 MHz) with a relationship with H_k; b) High frequency Q-factor (fitting data) of as-deposited CZTB lamination stack with dielectric material of AlN 5nm, Al_2O_3 5nm, SiN 5nm; c) loss tangent and damping factor of all the CZTB stacks.

Magnetic core loss is one of the main losses in inductor devices, and thus an important factor influencing device performance. Magnetic loss tangent (tanδ = μ''/μ') is used to represent losses in the magnetic material at high frequencies [O'Mathuna 2012]. Q-factor is defined as 1/ tanδ. Higher Q-factor means lower loss. Fig. 5 b) show the Q-factor frequency spectra of CZTB stacks with four dielectric materials, where AlN has the highest value, SiN and O-CZTB have medium Q-factor. The frequency response of the permeability can be theoretically analyzed by solving the Landau-Lifshitz-Gilbert (LLG) equation in combination with the Maxwell equations, which consider eddy-current loss contributions [Seemann 2010]. Damping factor of each sample can be estimated by LLG fitting. Figure 5. c) compares the damping factor α and measured loss tanδ. For CZTB stacks with same dielectric thickness (5nm) but different materials (AlN, SiN, Al_2O_3, O-CZTB), it can be seen that the loss tanδ follows the same variation trend with damping factor. CZTB stacks with AlN dielectric has the smallest damping factor and at the same time lowest magnetic high frequency loss. Samples with Al_2O_3 dielectric has the largest damping factor and highest loss tanδ. CZTB stacks with 5nm O-CZTB has both relatively high permeability and low loss (high Q-factor, which is 1/ tanδ). For CZTB stacks samples with same dielectric material (O-CZTB) but varied dielectric thickness (5, 15 and 50 nm), it can be observed that the magnetic loss tanδ is improved (decreasing) as thickness increases from 5 to 50 nm, while damping factor didn't change much. This can be explained by the depression of eddy current and displacement current losses using thicker dielectric layer. Previous publications [Wu 2012, Wang 2016] also showed that even with good quality dielectric separation layers, the loss tangent due to eddy and displacement current can become comparable or higher than damping losses, at high MHz frequencies.

IV. CONCLUSION

In this work, we have studied the effect of different dielectric materials (5 nm of AlN, SiN, Al_2O_3, and OCZTB) and different dielectric thicknesses (OCZTB; 5, 15 and 50 nm) on the static and dynamic magnetic behaviors of CZTB-based laminated stacks. Four major conclusions can be drawn as below: (i) Larger dielectric layer roughness will result in higher hard axis coercivity H_c, thus increasing the hysteresis loss. AlN dielectric material shows the best smoothness and a very low H_c; CZTB stack with 5 nm OCZTB also has a very low H_c; (ii) Higher stack residual stress can explain the larger induced magnetic anisotropy field H_k. Magnetic laminated stacks with SiN, or Al_2O_3 has the lowest stress thus the smallest H_k value; (iii) As the permeability value is in inverse relationship with H_k. CZTB stacks with AlN have the highest H_k and lowest permeability; (iv) Damping factor and eddy & displacement current are the main contribution to the high frequency magnetic losses. A higher damping factor will result in higher magnetic resonance loss. Higher dielectric thickness can weaken eddy and displacement current, thus decreasing the loss tangent. CZTB stacks with O-CZTB 5 nm dielectric, can be patterned using wet etching and exhibit a high permeability, low losses at high frequency, and a low H_c. and hence are an excellent choice for the fabrication of integrated inductors used in power conversion.

ACKNOWLEDGMENT

This work was supported by the project funding support from TEL (Tokyo Electron) Magnetic Solutions Ltd. and through Enterprise Ireland - Innovation Partnership Programme Contract No: EI-IP20200912.

REFERENCES

O'Mathuna C, Wang N, Kulkarni S, Roy S (2012), "Review of Integrated Magnetics for Power Supply on Chip (PwrSoC)," *IEEE Transactions on Power Electronics*, vol. 27, no. 11, pp. 4799-4816, doi: 10.1109/TPEL.2012.2198891.

Lambert W J, Hill M J, O'Brien K P, Radhakrishnan K, Fischer P (2020), "Study of Thin-Film Magnetic Inductors Applied to Integrated Voltage Regulators," *IEEE Transactions on Power Electronics*, vol. 35, no. 6, pp. 6208-6220, doi: 10.1109/TPEL.2019.2948825.

Ikeda S, Nagae T, Shimada Y, Kim K H, Yamaguchi M (2006), "Micropatterned high permeability films with narrow bandwidth resonance loss for the band stop filter," *J. Appl. Phys*., vol. 99, no. 8, pp. 08P507, doi: 10.1063/1.2171950.

Fergen I, Seemann K, Weth A V D, Schüppen A (2002), "Soft ferromagnetic thin films for high frequency applications," *J. Magn. Magn. Mater*., Vol. 242-245, pp. 146-151, doi: 10.1016/S0304-8853(01)01185-4.

Dinulovic D, Shousha M, Haug M (2020), "Microtransformer on silicon with CoFeB magnetic core for high-frequency signal applications," *AIP Adv*., vol. 10, pp. 015206, doi: 10.1063/1.5130009.

Wang N, Doris B B, Shehata A B, O'Sullivan E J, Brown S L, Rossnagel S, Ott J, Gignac L, Massouras M, Romankiw L T, Deligianni H L (2016), "High-Q magnetic inductors for high efficiency on-chip power conversion," 2016 IEEE International Electron Devices Meeting (IEDM), San Francisco, CA, USA, pp. 35.3.1-35.3.4, doi: 10.1109/IEDM.2016.7838547.

Wu H, Gardner D S, Xu W, Yu H (2012), "Integrated RF On-Chip Inductors With Patterned Co-Zr-Ta-B Films," *IEEE Trans. Mag*., vol. 48, no. 11, pp. 4123-4126, doi: 10.1109/TMAG.2012.2198448.

Yao D, Levey C G, Sullivan C R (2011), "Microfabricated V-groove power inductors using multilayer Co-Zr-O thin films for very-high-frequency DC-DC converters," *2011 IEEE Energy Conversion Congress and Exposition*, Phoenix, AZ, USA, 2011, pp. 1845-1852, doi: 10.1109/ECCE.2011.6064010.

Masood A, McCloskey P, O'Mathuna C, Kulkarni S (2018), "Co-based amorphous thin films on silicon with soft magnetic properties," AIP Adv., vol 8, pp. 056109, doi: 10.1063/1.5007733.

Jordan D, Wei G, Ye L, Lordan D, Podder P, Masood A, Rodgers K, O'Mathuna C, McCloskey P (2021), "High Q-Factor PCB Embedded Flip-Chip Inductors With Multilayer CZTB Magnetic Sheet for Power Supply in Package (PwrSiP)," *IEEE Trans. Emerg. Sel. Topics Power Electron*., vol. 9, no. 1, pp. 102-110, doi: 10.1109/JESTPE.2020.2983125.

Michel J P, Sibuet H, Buffet N, Bastien J C, Hida R, Viala B, Poveda P, Berneux-Dugast A S, Bruno E, Falub C V (2019), "Ultra-Low Profile Integrated Magnetic Inductors and Transformers for HF Applications," *IEEE Trans. Mag*., vol. 55, no. 7, pp. 1-7, doi: 10.1109/TMAG.2019.2905985.

Nosenko A V, Kyrylchuk V V, Semen'ko M P, Nowicki M, Marusenkov A, Mika T M, Semyrga O M, Zelinska G M, Nosenko V K (2020), "Soft magnetic cobalt based amorphous alloys with low saturation induction," *J. Magn. Magn. Mater*., vol. 515, pp. 167328, doi: 10.1016/j.jmmm.2020.167328.

Lordan D, Wei G, McCloskey P, O'Mathuna C, Masood A (2021), "Origin of perpendicular magnetic anisotropy in amorphous thin films," *Sci. Rep*., vol. 11, pp. 3734, doi: 10.1038/s41598-020-78950-7.

Bharadwaj S S, Rajkumar G R, Shivaraj B W, Krishna M (2017), "Effect of RF Sputtering Process Parameters on Silicon Nitride Thin Film Deposition," arXiv:1711.09556.

Wei G, Das R, Lordan D, Sai R, Hayes M, Lorenc M, Clarke B, Hurley D, McCloskey P (2023), "Development of CoZrTaB laminated thin films with novel CMOS compatible dielectric material," *IEEE Trans. Mag*., in print, doi: 10.1109/TMAG.2023.3287135.

Pal P, Swarnalatha V, Rao A V N, Pandey A K, Tanaka H, Sato K (2021), "High speed silicon wet anisotropic etching for applications in bulk micromachining: a review," Micro and Nano Systems Letters, vol. 9, no. 4, doi: 10.1186/s40486-021-00129-0.

Raju S, Neelakantan N, Soh S, Ho D, Singh R P (2020), "Thin-Film Magnetic Inductor Design Strategy for Integrated Voltage Regulator," *2020 IEEE 22nd Electronics Packaging Technology Conference (EPTC)*, Singapore, Singapore, pp. 159-161, doi: 10.1109/EPTC50525.2020.9315027.

Wang N, Zhou H, Zhang Z, Peng S, Yu J, Liao Z, Cheng M, Feeney C, Liu L, Ye T (2021), "A Novel Thin Film Cascade Matrix Coupled Inductor for Integrated Voltage Regulators," *IEEE Trans. Power Electron*., vol. 36, no. 12, pp. 13349-13354, doi: 10.1109/TPEL.2021.3087529.

Dubuget V, Dubourg S, Thibaudeau P, Duverger F (2010), "Magnetic Anisotropy Dispersion With Exchange Energy in Soft Ferromagnetic Thin Films," *IEEE Trans. Mag*., vol. 46, no. 5, pp. 1139-1142, doi: 10.1109/TMAG.2010.2040187.

Ghaferi Z, McCloskey P (2020), "Characterization and enhancement of magnetic performance of electrodeposited Ni45Fe55 on PCB for high frequency application," *J. Magn. Magn. Mater*., vol. 505, pp. 166708, doi: 10.1016/j.jmmm.2020.166708.

Jordan D, Wei G, Ghaferi Z, Masood A, O'Mathuna C, McCloskey P (2020), "Stochastic magnetic resonance of absorption effects of surface morphology in thin film magnetics,"*J. Magn. Magn. Mater*., vol. 505, pp. 166736, doi: 10.1016/j.jmmm.2020.166736.

Cronin D, Lordan D, Wei G, McCloskey P, O'Mathúna C, Masood A (2020), "Soft magnetic nanocomposite CoZrTaB–SiO2 thin films for high-frequency applications," *J. Appl. Phys*., vol. 127, pp. 243903, doi: 10.1063/5.0013416.

Zhukova V, Churyukanova M, Kaloshkin S, Corte-Leon P, Ipatov M, Zhukov A (2023), "Magnetostriction of amorphous Co-based and Fe-Ni-based magnetic microwires: Effect of stresses and annealing," *J. Alloy. Compd*., vol. 954, pp. 170122, doi: 10.1016/j.jallcom.2023.170122.

Seemann K, Leiste H, Klever C (2010), "Determination of intrinsic FMR line broadening in ferromagnetic $(Fe_{44}Co_{56})_{77}Hf_{12}N_{11}$ nanocomposite films," *J. Magn. Magn. Mater*., vol. 322, pp. 2979-2983, doi:10.1016/j.jmmm.2010.05.062.

Hamzehbahmani H, Anderson P, Hall J, Fox D (2014), "Eddy Current Loss Estimation of Edge Burr-Affected Magnetic Laminations Based on Equivalent Electrical Network—Part I: Fundamental Concepts and FEM Modeling," *IEEE Trans. Power Delivery*, vol. 29, no. 2, pp. 642-650, doi: 10.1109/TPWRD.2013.2272663.

Yao D, Sullivan C R (2009), "Calculation of eddy-current loss in multilayer magnetic films considering displacement current," J. App. Phys., vol. 105, no. 7, pp. 07A335, doi: 10.1063/1.3074134.